International Wound Journal

WILEY

IWJ

ORIGINAL ARTICLE OPEN ACCESS

The Protective Efficacy of a New Soft Silicone Multi-Layer Dressing in Reducing the Heel Pressure Ulcer Risk

Daria Orlova[1] | Aleksei Orlov[1] | Amit Gefen[1,2,3]

[1]School of Biomedical Engineering, Faculty of Engineering, Tel Aviv University, Tel Aviv, Israel | [2]Skin Integrity Research Group (SKINT), University Centre for Nursing and Midwifery, Department of Public Health and Primary Care, Ghent University, Ghent, Belgium | [3]Department of Mathematics and Statistics and the Data Science Institute, Faculty of Sciences, Hasselt University, Hasselt, Belgium

Correspondence: Amit Gefen (gefen@tauex.tau.ac.il)

Received: 30 June 2025 | **Revised:** 4 September 2025 | **Accepted:** 11 September 2025

Funding: This work was supported by Smith & Nephew Limited, Hull, United Kingdom.

Keywords: ALLEVYN COMPLETE CARE | computational finite element modelling | friction and shear mitigation | frictional energy absorber effectiveness | pressure injury prevention/prophylaxis

ABSTRACT

Soft silicone multi-layer dressings are commonly used for pressure ulcer (pressure injury) prevention, yet their effectiveness varies based on design, construct, and material properties. This study evaluated the protective efficacy of a new multi-layer dressing, ALLEVYN COMPLETE CARE (ACC, Smith & Nephew Limited), which incorporates an advanced structure facilitating the dissipation of shear forces through internal layer-on-layer frictional sliding within the dressing. Using a combination of experimental frictional energy absorber effectiveness (FEAE) testing and computational finite element modelling, we quantified the capacity of this dressing to mitigate strain and stress concentrations in the soft tissues of the supported posterior heel. The dressing demonstrated considerable frictional sliding between its adjacent layers, resulting in FEAE = 93% under simulated, clinically relevant usage conditions. This was associated with the dissipation of shear forces and alleviation of strain/stress concentrations in the skin and underlying soft tissues below the dressing. The dressing completely eliminated the stress and strain peaks at the top quartiles of the strain/stress domain (with reference to a no-dressing case). This work provided valuable insights into advanced testing methods and beneficial design principles for pressure ulcer prevention dressings. Earlier investigations concluded that a previous-generation ALLEVYN LIFE dressing achieved high levels of FEAE and thus provided protection. Our findings here establish that the next-generation dressing, ACC, demonstrates even greater protective capacity.

1 | Introduction

The heel remains a prevalent anatomical site for the formation of a pressure ulcer (PU), also termed (heel) pressure injury, with some of these wounds initially developing as deep tissue injuries that later present themselves as open wounds. Through this pathogenesis, soft tissue damage begins and progresses below intact skin and is challenging to timely diagnose and clinically classify [1, 2]. It is only after the breakdown of the skin that the extent of tissue destruction becomes apparent and is typically classified as full-thickness tissue damage. For this reason, it is critically important to protect the heels of patients who are categorised as being at risk. Current international clinical practise guidelines recommend the use of prophylactic dressings, particularly multi-layer foam constructs, on high-risk anatomical sites such as the heels and sacrum to support pressure ulcer prevention [3–6]. In response, manufacturers have developed soft silicone multi-layer dressings specifically contoured to fit the heel

Abbreviations: ACC, ALLEVYN complete care; ANOVA, analysis of variance; COF, coefficient of friction; FE, finite element; FEAE, frictional energy absorber effectiveness; MOA, mode of action; PEI, protective efficacy index; PU, pressure ulcer; PUP, pressure ulcer prevention; ROI, region of interest.

Summary

- The heel remains a prevalent anatomical site for formation of pressure ulcers.
- A new soft silicone multi-layer dressing was evaluated for injury prevention.
- This dressing demonstrated high frictional energy absorber effectiveness.
- Computational finite element modelling confirmed alleviation of tissue loading.
- We demonstrated advanced testing methods and design principles for prophylaxis.

anatomy [3, 4, 7]. Several dressing types are currently applied to at-risk patients in acute (e.g., critical care and operating room) settings, following national and international guidelines recommending this preventative intervention.

Using an animal model coupled with computational simulations, the pioneering work of Ceelen and colleagues linked the distribution of mechanical strains in soft tissues with the risk of injury onset. Their combined experimental-numerical approach demonstrated a reproducible, monotonic increase in tissue damage with increasing maximum shear strain, once a critical strain threshold was exceeded [8]. With this progress and basic science and the appearance of dressings indicated for pressure ulcer prevention (PUP) in the wound care market, approximately a decade ago, the senior author and his research group initiated the development of relevant bioengineering laboratory testing methods (which were nonexistent at the time), following a strategy aimed at allowing clinicians and other stakeholders to be better informed when selecting their PUP dressings [9–11]. These methods were designed for methodological evaluations of the protective efficacy of PUP dressings in a standardised and quantitative manner, similarly to fluid handling performance testing in a treatment context [12, 13]. Whilst being advanced, they were also practical to implement by the dressing industry, which adopted them in multiple works evaluating the products of different majors [9–12, 14–19]. The focus of these testing methods was to assess the ability of a preventative dressing to positively impact the state of soft tissue loading during supported body postures (or under skin-contacting medical devices), typically by redistributing the bodyweight forces (or the device-applied loads) to avoid stress and strain concentrations, so that the tissues below the dressing are eventually exposed to lower mechanical loading levels. In this context, central to the effectiveness of preventative multi-layer dressings is their ability to dissipate the frictional forces through a phenomenon termed by the senior author as the 'frictional energy absorber effectiveness' (FEAE), which essentially quantifies the amount of friction and shear-related mechanical energy absorbed within the dressing itself, rather than transmitted to the skin and from there, to the underlying soft tissues of the patient [9]. Our published work already demonstrated that the FEAE mode of action (MOA) is empirically measurable; that is, if a certain multi-layer dressing design facilitates layer-on-layer movements through unbonded pad layers, then the energy absorbed by the dressing through this MOA whilst external shear forces apply is quantifiable through a suitable laboratory measurement apparatus described in [9].

Based on our published work concerning the FEAE MOA [9], this study seeks to evaluate the protective efficacy of a newly designed, commercial multi-layer dressing, the ALLEVYN COMPLETE CARE (ACC), manufactured by Smith & Nephew Limited (Hull, United Kingdom), which is a second generation to their market-popular ALLEVYN LIFE dressing. The empirical FEAE testing method described in detail in [9] was therefore combined here with advanced computational modelling, considering, for the first time in the literature, the frictional sliding interactions within the dressing layers, and their effects on the tissue loading state in the anatomically realistically modelled, supported posterior heel. The latter phenomenon was further investigated using the protective efficacy index (PEI) measure, also developed and implemented by our research group [11, 12, 14–19]. By assessing both the FEAE and PEI metrics of the new ACC dressing, we quantified its capacity to absorb mechanical energy internally within its construct, and consequently, its ability to alleviate strain and stress concentrations in skin and underlying soft tissues under simulated, clinically relevant conditions. This research approach, which combines advanced in vitro and in silico laboratory testing, provides a comprehensive and contemporary view of how dressings should be assessed for their PUP performance from a bioengineering perspective. Specifically, the currently employed methods evaluate the ability of the ACC dressing to protect at-risk patients from heel PUs and identify the MOA by which this dressing design achieves its protective effect.

2 | Materials and Methods

2.1 | Frictional Energy Absorber Effectiveness Measurements

The FEAE performance measure focuses on the amount of mechanical energy absorbed internally within a multi-layer dressing during preventative use, as adjacent layers of the dressing slide frictionally over each other. The energy absorbed internally in the dressing, as quantified by the FEAE, mitigates the transfer of damaging shear forces to the skin and subcutaneous tissues [9], and has been shown in recent computational studies to reduce shear strain cluster volumes in the soft tissues within the region of interest (ROI) [20, 21]. This method of analysis was applied to the new dressing design to evaluate its biomechanical protective efficacy compared to the formerly tested (previous-generation) dressing design [9], and further combine it with computational finite element (FE) modelling to bridge between the non-anatomical FEAE test configuration [9] and the anatomical arrangement and biomechanical behaviour and properties of the relevant soft tissues.

The FEAE measurements in this study were conducted exactly as described in [9], using the same test setup to allow direct comparisons between the performance of the new dressing design and the previously tested dressing type. The FEAE measurement method is briefly summarised here for completeness. For detailed information, including theoretical formulation, definitions of energy terms, and calculation procedures, readers are referred to Marché

et al. [9] and to Appendix A of the current work, which provides a concise summary of the original FEAE methodology. The dressing layers of interest are referred to as follows: hydrocellular foam ($i=2$), which is bonded to the silicone adhesive layer; the hyper-absorber layer with gelling fibres ($i=3$); and the breathable protective layer ($i=4$), which is bonded to the external masking film. The coefficient of friction (COF) values ($\mu_{i,i+1}$) and inter-layer displacements ($d_{i,i+1}$) were studied at the two relevant inner interfaces, #2 & #3 and #3 & #4, where frictional sliding may occur (Table 1). Since layer #2 is bonded to the silicone adhesive, which in turn adheres to the skin, we assumed no frictional sliding at these interfaces and did not consider them as contributing to the FEAE.

Two testing conditions were defined, namely, new/dry (out-of-the-package) and used/moist (accounting for exposure to perspiration and repetitive shearing expected with wear), the latter representing clinically relevant conditions applying after a short period of use (considering that dressings used for PUP are typically applied for periods of several days). To induce the used/moist condition, the dressing specimens were left overnight, for 7 h, on a moist, semi-permeable chamois cloth sprayed with a 0.9% saline solution simulating sweaty skin. The specimens then underwent 10 loading cycles of combined compression (via a 1.1 kg vertical mass) and shear (increasing to 1 kg at 50 mm travel speed). Then, 10 loading cycles of coupled compression (exerted by a 1.1 kg mass) and shear stress (increasing up to 1 kg delivered at a speed of 50 mm) were applied to these specimens, following which the $\mu_{i,i+1}$ and $d_{i,i+1}$ data were acquired for calculating the used/moist FEAE [9].

Inter-layer sliding displacements $d_{i,i+1}$, in particular, were measured using a high-resolution optical method. Fiducial markers were sprayed onto the exposed cross-sections of each dressing layer and tracked using digital image correlation (DIC), based on DSLR photography and a custom MATLAB algorithm. Displacements were recorded at the point of maximum shear force before sliding (approximately 6 N). This technique captures the local relative motion between adjacent layers, independent of global specimen movement. Whilst the experimental setup used force-controlled shear under fixed compression, the FE simulations applied displacement-controlled boundary conditions to reproduce the equivalent kinematic state at slip onset. Importantly, what is compared between the two modalities is not the absolute load or displacement, but the relative sliding between layers under clinically relevant conditions. Although the use of force versus displacement control may affect reaction forces due to boundary stiffness, the local kinematics and energy-dissipating behaviour of the dressing remain robust and comparable across both platforms.

TABLE 1 | Contact conditions between adjacent components in the finite element model variants.

Model variant	Contact pair	Contact type	COF
No dressing case	Skin and support surface	Frictional	0.43
Dressing case	Skin and dressing layer #1	Tied	—
	Dressing layers #2 and #3	Frictional	0.78
	Dressing layers #3 and #4	Frictional	0.98
	Dressing layer #5 and support surface	Frictional	0.35

Abbreviation: COF, coefficient of friction.

Having established the biomechanical efficacy of the new dressing design experimentally through these FEAE studies, we proceeded to computational modelling to further investigate the heel tissue interactions with this dressing in an anatomical configuration, as detailed below.

2.2 | Computational Modelling and Simulations

2.2.1 | Geometrical Features and Mechanical Properties of the Model Components

Two FE model variants of the posterior left heel resting on a flat medical foam support surface were developed using the anatomically accurate, MRI-based FE modelling framework described in detail in our previously published work [10], now studied without and with the applied new dressing. The heel anatomy was identical in the two current model variants and included the posterior calcaneus, calcaneal tendon, adipose, and skin tissues (Figure 1a). The new dressing design is composed of five layers; however, the respective model variant included the core dressing layers relevant to the FEAE evaluation, that is, all the inner layers between which frictional sliding occurs, namely, layers #2, #3, and #4 (Table 1), with thicknesses of 1.9 mm, 2.5 mm, and 0.35 mm, respectively (i.e., total dressing thickness of 4.75 mm) (Figure 1b). The skin-facing silicone layer #1 and the masking film #5 that opposes the support surface are considerably thinner than the middle layers (#2, #3, and #4), and given their negligible thickness, were not modelled as distinct physical entities. Instead, their effects were accounted for through contact conditions (Table 1). The support surface was modelled to a depth of 10 mm for computational efficiency.

The mechanical properties of the heel tissues were derived from widely used finite element studies of lower-limb anatomy, particularly those focused on pressure ulcer prevention [10, 22–23]. The soft tissues (skin and adipose) were modelled using compressible Neo-Hookean material definitions, where the long-term (equilibrium) shear modulus (G) and bulk modulus (K) were taken directly from literature and converted to Abaqus input parameters as C_{10} and D_1. The Achilles tendon and calcaneus bone were modelled as linear elastic materials using elastic moduli and Poisson's ratios from the same literature sources. These parameters fall within the range reported in the literature. For example, Levy and Gefen [10] reported heel skin shear moduli ranging from approximately 30–220 kPa, depending on anatomical region and loading condition, whilst Sopher et al. [22] reported adipose tissue shear moduli near 0.28–0.29 kPa under the assumption of near-incompressibility. Importantly, this dataset leads to model-predicted tissue strains of ~20%–30% in the absence of a dressing, consistent with prior validated heel models and conservative from a PUP standpoint. A more compliant skin choice yields higher tissue strains, challenging the dressing and ensuring that protection is not overestimated.

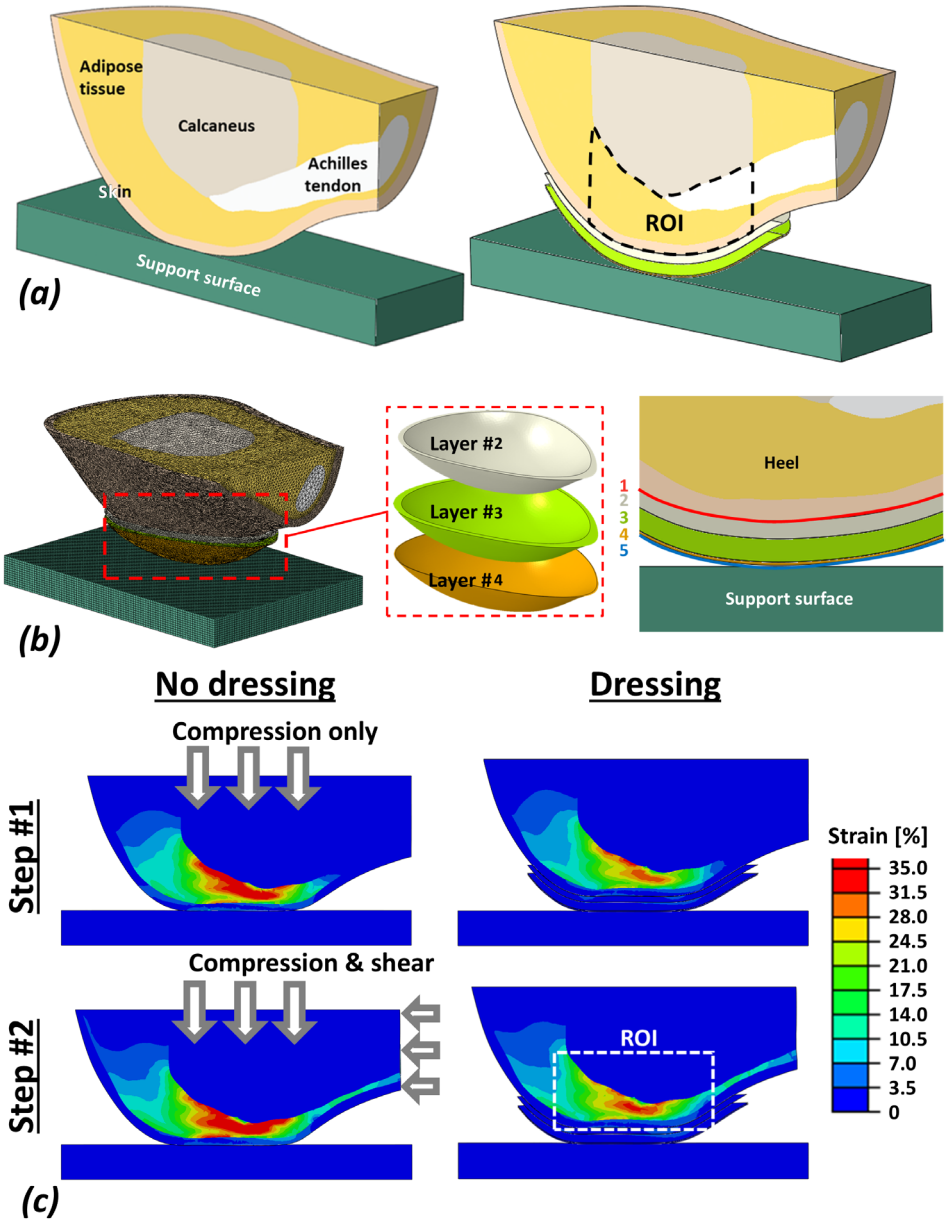

FIGURE 1 | The finite element model of the heel (a) with its components (left panel) and the region of interest (ROI) marked in dashed black lines (right panel) used to calculate the computational outcome measures after (b) meshing of the model components (left panel), including the support surface and the dressing layers considered to have physical thickness in the model (center and right panels). The model was solved for the internal loading state in the tissues and the ALLEVYN COMPLETE CARE (Smith & Nephew Limited) dressing in a two-step process, simulating first positioning and then sliding in bed (as when the head of the bed is elevated). In step #1 only the compressive force of the foot weight was applied (top row) and in step #2 shear was added (bottom row). The resulting strain distributions in the soft tissues of a sagittal cross-section through the posterior heel are shown in (c) for the model variants without dressing (left column) and with the dressing applied prophylactically (right column), and for step #1 (effective strains) and step #2 (maximal shear strains).

The constitutive models and mechanical properties of all tissues were as in our published work [10] and are specified in Table 2 for completeness. The stiffnesses of each dressing layer considered to have physical thickness (#2, #3, #4) were measured under unconfined compression by means of an electromechanical uniaxial testing system (INSTRON Co. model 5544, High Wycombe, UK) at a quasi-static displacement rate of 12 ± 3 mm/min, in a ramp-and-hold loading mode up to a compressive strain of 50% to assess viscoelastic properties. The instantaneous elastic moduli E_{ins} were calculated per each core dressing layer #2, #3 and #4 by linear approximation of the stress–strain curves in the final 25% strain range of the 'ramp' phase, which reflects the large deformations of dressing materials expected during clinical use [10]. A stress relaxation curve was plotted next for the 'hold' phase per each trial and for each layer #2, #3 and #4. Finally, the long-term compressive elastic moduli E_{lt} of each layer #2, #3 and #4 were calculated by averaging the last 25% of the stress-time (i.e., the stress relaxation) curve. The E_{ins}/E_{lt} ratios were approximately 1.6 ± 0.1 for layer #2 and 1.1 ± 0.1 for layers #3 and #4, which indicates a non-negligible viscoelastic behaviour of these dressing materials.[1] Furthermore, we observed relatively short viscoelastic relaxation times for all these

TABLE 2 | Mechanical properties and mesh discretization for components of the finite element FE model: Heel, ALLEVYN COMPLETE CARE dressing, and support surface.

Component	Material type	Elastic modulus E (kPa)	Poisson's ratio ν	Material parameter C_{10} (kPa)	Compressibility parameter D_1 (kPa)	Nodes	Elements	DOFs
Calcaneus bone [10, 22, 24]	Elastic	7×10^6	0.3	—	—	8346	34446	59484
Achilles tendon [10, 22, 24]	Elastic	205	0.49	—	—	4059	13869	26046
Adipose tissue [10, 24]	Hyperelastic	—	—	0.14	0.07	69158	282267	489741
Skin	Hyperelastic	—	—	15.95	6.3×10^{-4}	90476	324385	595813
Dressing layer #2	Elastic	8.0	0.3	—	—	12287	48509	85370
Dressing layer #3	Elastic	34.1	0.3	—	—	14601	62946	106749
Dressing layer #4	Elastic	1310.7	0.3	—	—	8596	25206	50994
Support surface	Elastic	45	0.3	—	—	156996	143000	470988

Abbreviation: DOFs, degrees of freedom.

materials, of approximately up to 5 min, compared to the typical timeframes for the development of PUs. Overall, the above experimental results indicated that the long-term elastic moduli E_{lt} are the appropriate stiffness characteristics of the studied dressing for the purpose of the FE modelling. Accordingly, these E_{lt} data were the dressing stiffness (elastic modulus) values which were listed in Table 2, and that were also further used for the modelling work reported as follows.

2.2.2 | Boundary and Loading Conditions

The boundary conditions applied to the FE model of the heel were selected to simulate the positioning of a supine patient on a support surface, followed by sliding or movement in bed as may occur, for example, if the head of the bed is elevated or if the patient is being repositioned. Consistent with our published work [10], we applied a vertical displacement of 4 mm on the superior surface of the calcaneal bone, followed by a 3.5 mm horizontal displacement of the same surface (Figure 1c). These displacement-controlled boundary conditions were selected because the calibration targets and experimental observables in both our current and prior works [10] are kinematic in nature. This approach ensures that all support surface or dressing variants experience the same deformation pattern, which would not be possible with force-controlled inputs. Displacement control allows us to reproduce a consistent weight-bearing configuration whilst facilitating direct comparisons of inter-layer sliding and tissue loading across model variants. It also provides improved numerical stability near slip initiation, as force control could lead to unpredictable displacements and convergence difficulties when local stiffness varies. This modelling strategy therefore supports both mechanical relevance and computational robustness. The bottom aspect of the support surface was constrained for both translation and rotation, and tied interfaces were applied between all tissue components in the model. The COF between the bare skin and the support surface (assumed to be covered by cotton bedlinen) was set at 0.43 to represent typical dynamic friction of skin with cotton sheet. The inter-layer COFs for the studied dressing were measured experimentally (as an integral part of the FEAE evaluation process described in [9]) using a tilting table tribometer, following the method described in [9], and mean values (Figure 2a) used for the FE model variant with the dressing are reported in Table 1. The COF of the external dressing surface (masking film layer #5) with cotton sheet was measured as well using the same tribometer and found to be 0.35 ± 0.04 (Table 1).

2.2.3 | Numerical Methods and Computational Outcome Measures

Meshing of the tissues was performed using the ScanIP module of Simpleware (version R-2021.03) with a finer mesh employed within the entire skin volume, and particularly in skin areas contacting the dressing or support surface. The meshes for the dressing and support surface were generated in Abaqus/CAE 2023, whilst carefully maintaining consistency in element type and size with respect to the heel mesh. The calcaneus, AT, adipose tissue, skin, and all dressing layers were meshed using four-node linear tetrahedral elements with hybrid formulation (C3D4H), whilst the support surface was meshed using eight-node linear brick elements with reduced integration and hourglass control (C3D8R). Both element types offer computational efficiency for compressible materials. The number of nodes and elements for each component is provided in Table 2.

All the FE simulations were conducted by means of the Abaqus/CAE 2023 software suite using its standard static solver for non-linear, large deformation problems. Each model variant required approximately 2 h to process on a 64-bit Windows 10 workstation with an Intel Core i9-7900X CPU (3.30 GHz) and 64 GB RAM, which is typical runtime for the computational complexity of the current modelling framework.

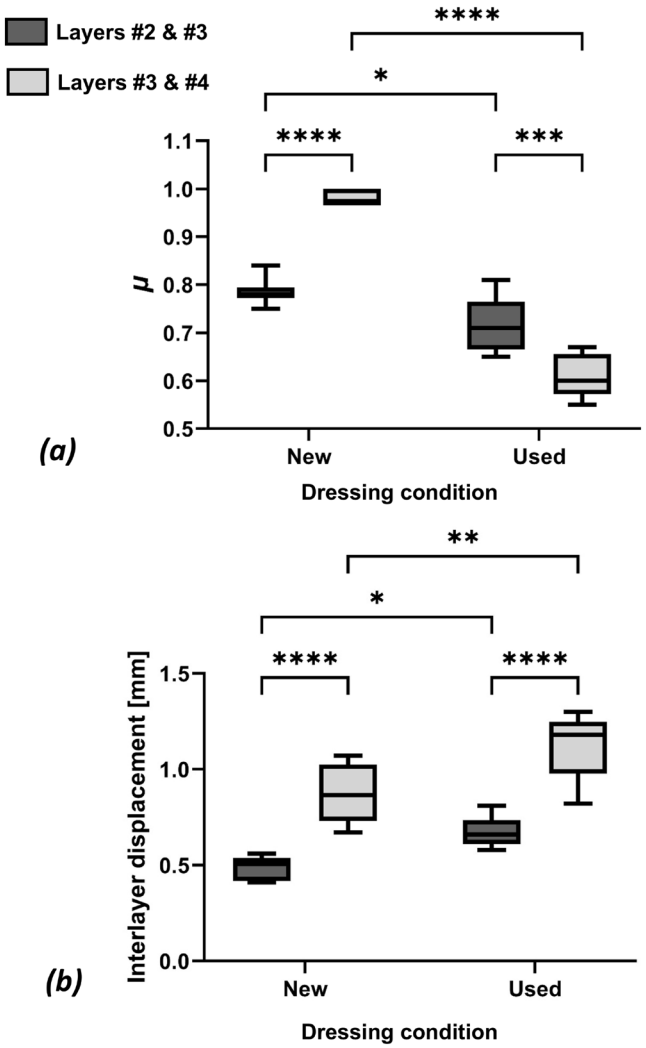

FIGURE 2 | Boxplots showing the effect of condition (used versus new) on the interlayer (a) coefficient of friction (μ) and (b) displacement values in the tested ALLEVYN COMPLETE CARE (Smith & Nephew Limited) dressing, which were used to calculate the frictional energy absorber effectiveness (FEAE) outcome measure (the values are also specified in Table 3). *$p < 0.05$, **$p < 0.01$, ***$p < 0.001$, ****$p < 0.0001$.

We evaluated the volumetric exposure of the soft tissues in the posterior heel to sustained mechanical loading, specifically in terms of tissue strain and stress distributions. These data were obtained for the skin, adipose tissue, and tendon within a defined ROI. The ROI was delineated as the soft tissue wedge directly beneath the calcaneus, bounded inferiorly by the dressing and superiorly by the retro-calcaneal projection of the bone (Figure 1a). This included only the skin and subcutaneous adipose tissue within the dressing—tissue contact footprint, whilst bone and tendon tissues were excluded.

This definition was chosen because heel pressure ulcers are understood to originate in the deformable soft tissues, particularly adipose and skin, rather than in stiffer structures such as tendon. Focusing the ROI and metric extraction on this soft tissue wedge improves the relevance of our results by targeting the tissues most susceptible to mechanical damage under sustained compression and shear. It also avoids diluting the strain and stress distributions with low-loaded peripheral regions. This ROI selection is consistent with previous FE studies of the foot and prophylactic interventions, as reviewed by Keenan et al. [25].

In all finite element analyses reported in this study, tissue deformations were quantified using the maximum principal logarithmic strain (LE), extracted from the output database of Abaqus. The logarithmic strain measure was selected to accommodate the relatively large tissue deformations simulated here and to ensure accurate strain representation across both loading steps—compression and shear. Maximum principal strain reflects the greatest normal stretch experienced at a material point, independent of direction, and is biomechanically meaningful because excessive sustained deformation is a known driver of cell death and soft tissue breakdown in pressure ulcer aetiology.

Indeed, elevated principal strain levels have been strongly associated with deep tissue injury in animal-computational studies coupling histological damage with simulated mechanical strain fields [8, 26]. Therefore, all strain-based analyses and PEI calculations (Appendix B) in this study were based solely on the LE-based maximum principal strain.

Whilst von Mises stresses were also evaluated to provide complementary insights (i.e., accounting for tissue stiffness and volumetric loading), the strain metrics remain the primary focus given their direct pathophysiological relevance to sustained loading damage in PUP scenarios.

Histograms were generated to illustrate the distribution of strains and stresses in the skin, adipose tissue, and the combined heel soft tissues. To assess the protective efficacy of the dressing under investigation, we calculated its PEI based on both strain and stress exposures in the soft tissues within the ROI. The PEI, a performance metric developed by the senior author and widely used in the literature, has been applied in many studies on the efficacy of PUP measures such as different dressings and positioners [11]. In brief, the PEI quantifies how effectively a dressing used for PUP redistributes soft tissue loading in its surroundings, and in particular, how efficiently does it alleviates tissue strain and stress concentrations compared to a condition without the studied dressing. To calculate the PEI of the studied dressing, we generated histograms representing the distributions of strains and stresses in the soft tissues within the ROI for both model variants, without and with the dressing. We then computed the percentage difference in the areas under these histograms per tissue type, separately for strain and stress measures. A greater flattening of the histogram when using the dressing, compared to the no-dressing scenario, corresponds to a higher PEI, indicating better protective performance [11]. The PEI values were calculated for two different strain/stress domains: first, for the second to fourth quartiles (above 25%), which excluded lower strain and stress levels that occur naturally due to gravitational forces; and second, for the fourth quartile alone (above 75%), which focuses on the highest strain and stress concentrations in the tissues. These PEI analyses were conducted considering that the dressing materials remain microscopically intact during the intended period of clinical use and so, the stiffness properties of the layers remain consistent (although the frictional layer-on-layer interactions examined by FEAE are affected by moisture and repetitive shearing; Figure 2). This was

tested and confirmed experimentally by preconditioning the thickest and most vulnerable to microscopic tearing [13, 27] hyper-absorber layer with gelling fibres (layer #3) through moisture induction and repetitive shearing, according to the current FEAE study protocol [9]. Subjecting this layer to the mechanical testing described above (in Section 2.2.1) indicated no statistically significant differences in E_{ins} or E_{lt} due to the aforementioned preconditioning.

3 | Results

3.1 | Frictional Energy Absorber Effectiveness Studies

The performance of the studied dressing was evaluated experimentally by measuring the $\mu_{i,i+1}$ and $d_{i,i+1}$ for interfaces, #2 & #3 and #3 & #4 (Figure 2 and Table 3). In the new condition (out-of-the-package), the dressing exhibited greater COFs (at both interfaces), which decreased by 8% and 38% following simulated use (which included moisturising and shearing conditions), respectively (Figure 2a). Analysis of variance (ANOVA) followed by Tukey–Kramer pairwise comparisons indicated that these COF decreases were both statistically significant (Figure 2a). Prior to statistical analysis, all group residuals were assessed for normality using the Shapiro–Wilk test, and no departures from normal distribution were detected (Table A3). The groups were balanced ($n = 6$ per condition) and independent by design, supporting the assumptions for ANOVA. Given these conditions and the robustness of ANOVA to modest variance differences, the use of ANOVA and Tukey–Kramer comparisons was statistically justified. Consistent with the decreases of the COFs, both interlayer displacements significantly increased, 37% and 29% following the simulated use, respectively (Figure 2b). The $\mu_{i,i+1}$ and $d_{i,i+1}$ measurements indicated a statistically significant increase in frictional interlayer sliding with simulated use (Figure 2 and Table 3). The clinically relevant FEAE measure calculated from the $\mu_{i,i+1}$ and $d_{i,i+1}$ simulated use data, $93\% \pm 5\%$, indicated notable effectiveness of the new dressing design in absorbing shear internally within its sliding multi-layer structure (Table 3).

3.2 | Computational Studies

The effectiveness of the dressing under investigation in alleviating soft tissue loading within the supported posterior heel (as depicted in Figure 1c) was quantitatively investigated. Although not prominent at the full-model visualisation scale, the support surface experienced localised compression directly beneath the heel. Displacement contour plots focused on this region (Figure C1, Appendix C) revealed a maximum vertical settlement of approximately 4% strain. This is consistent with the material properties assigned to the support surface (Table 2) and the fact that the model used displacement-controlled loading, where most of the imposed 4 mm downward motion was absorbed by the dressing and soft tissues. Only a small portion of the compressive displacement propagated into the support surface. In the experimental setup, although the support platform was not instrumented to directly measure compression, visual inspection showed only minor deformation during FEAE testing, qualitatively aligning with the FE results. Thus, the support surface deformation predicted by the model is both mechanically plausible and experimentally consistent.

Histograms of soft tissue exposure to loading in the ROI revealed that the dressing substantially lowered all the above-median strains and stresses consistently for both skin and adipose tissues (Figure 3) and completely eliminated the strain and stress concentrations in the fourth quartiles of the respective domains (Figure 4). To further investigate how tissue loading evolves under shear, we plotted the average maximal principal strain and stress as a function of imposed shear displacement (Figure 5).

To quantify these trends, we computed the linear slope of each curve over the 0–3 mm shear displacement range using least-squares regression, separately for each ROI and condition (i.e., with and without dressing). Slope values with standard errors and 95% confidence intervals (CIs) are summarised in Table D1, and the fitted regression lines are shown in Figure D1.

The results confirmed that tissue loading increases more rapidly without the dressing. In skin, both strain and stress slopes under the ACC dressing were close to zero, with 95% CIs including zero, indicating flat or near-flat trends. In adipose tissue, strain increased more gradually with the dressing, whilst the no-dressing condition exhibited a noticeably steeper slope. Stress in adipose tissue remained relatively flat in both conditions.

To assess whether these slope differences were statistically significant, we performed extra-sum-of-squares F-tests (ANCOVA). Although slope values were consistently lower with the dressing, the differences were not statistically significant ($p > 0.05$), likely due to the limited displacement range and small effect sizes. Still, the consistent trends support the interpretation that the ACC dressing slows the rate of internal tissue loading during shear, consistent with its FEAE mechanism.

TABLE 3 | Parameter values used for calculating the frictional energy absorber effectiveness (FEAE) of the dressing under investigation.

Dressing condition	$\mu_{2,3}$	$\mu_{3,4}$	$d_{2,3}$ (mm)	$d_{3,4}$ (mm)	y (mm)	FEAE (%)
New	**0.78** (0.03)	**0.98** (0.01)	**0.49** (0.06)	**0.87** (0.15)	**1.23** (0.09)	**100** (13)
Used	**0.72** (0.06)	**0.61** (0.05)	**0.67** (0.08)	**1.12** (0.18)	**1.25** (0.15)	**93** (5)

Note: All values are provided as mean are in bold (standard deviation).

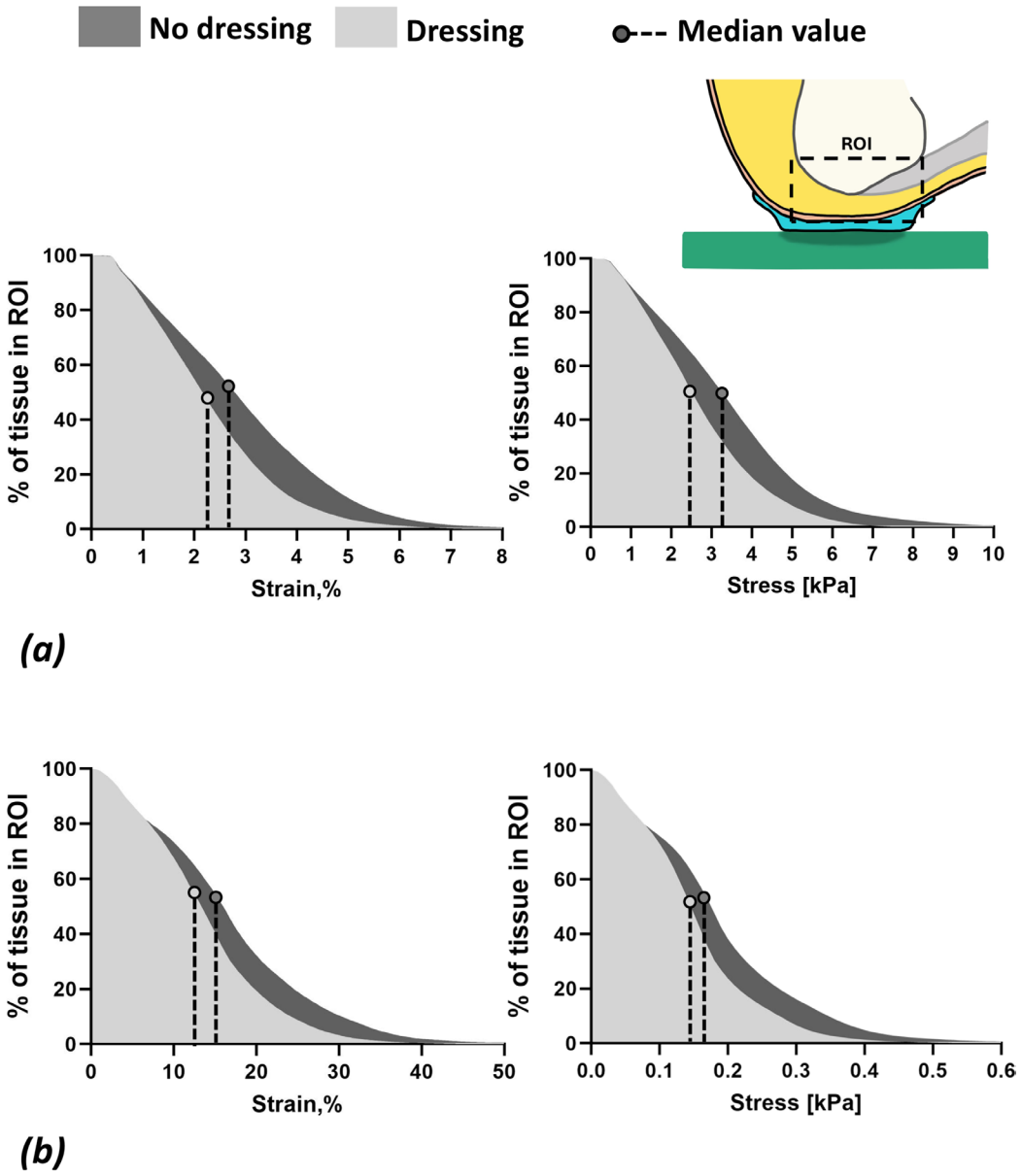

FIGURE 3 | Histograms showing soft tissue exposure to the full range of effective strains (left column) and stresses (right column) in the region of interest (ROI), comparing the ALLEVYN COMPLETE CARE (Smith & Nephew Limited) dressing to the no-dressing case, for (a) skin and (b) adipose tissues.

These findings suggest that during sliding events, the soft tissues in an unprotected heel experience not only higher strain and stress levels, but also a faster buildup of loading. In contrast, when the ACC dressing is applied, the tissue loading remains nearly unchanged throughout the shear displacement range, further supporting its protective effect.

The strain and stress distributions in the heel tissues (Figure 6) revealed that the highest values occurred approximately midway through the tissue depth, but these peaks were substantially reduced with the dressing. Finally, the PEI analyses demonstrated that the new dressing eliminated all above the 75th percentile strain and stress exposures and reduced those above the 25th percentile by ~55% (strain) and up to 92% (stress), as shown in Table 4.

4 | Discussion

In the current work, the ACC dressing demonstrated considerable biomechanical efficacy in mitigating the PU risk under clinically relevant conditions, i.e., the induced mechanical preconditioning and moist states which mimic real-world use. This laboratory study assessed the FEAE experimentally and the PEI computationally, and these outcome measures collectively define the protective performance in at-risk body areas such as the heel. Our findings suggest that the unique structure with able-to-slide layers and mechanical properties of the ACC dressing, and in particular, the interlayer relative movement occurring as shear forces apply, enables effective shear dissipation within the dressing and redistribution of elevated stresses within the tissues, including under the expected moisture exposure. This

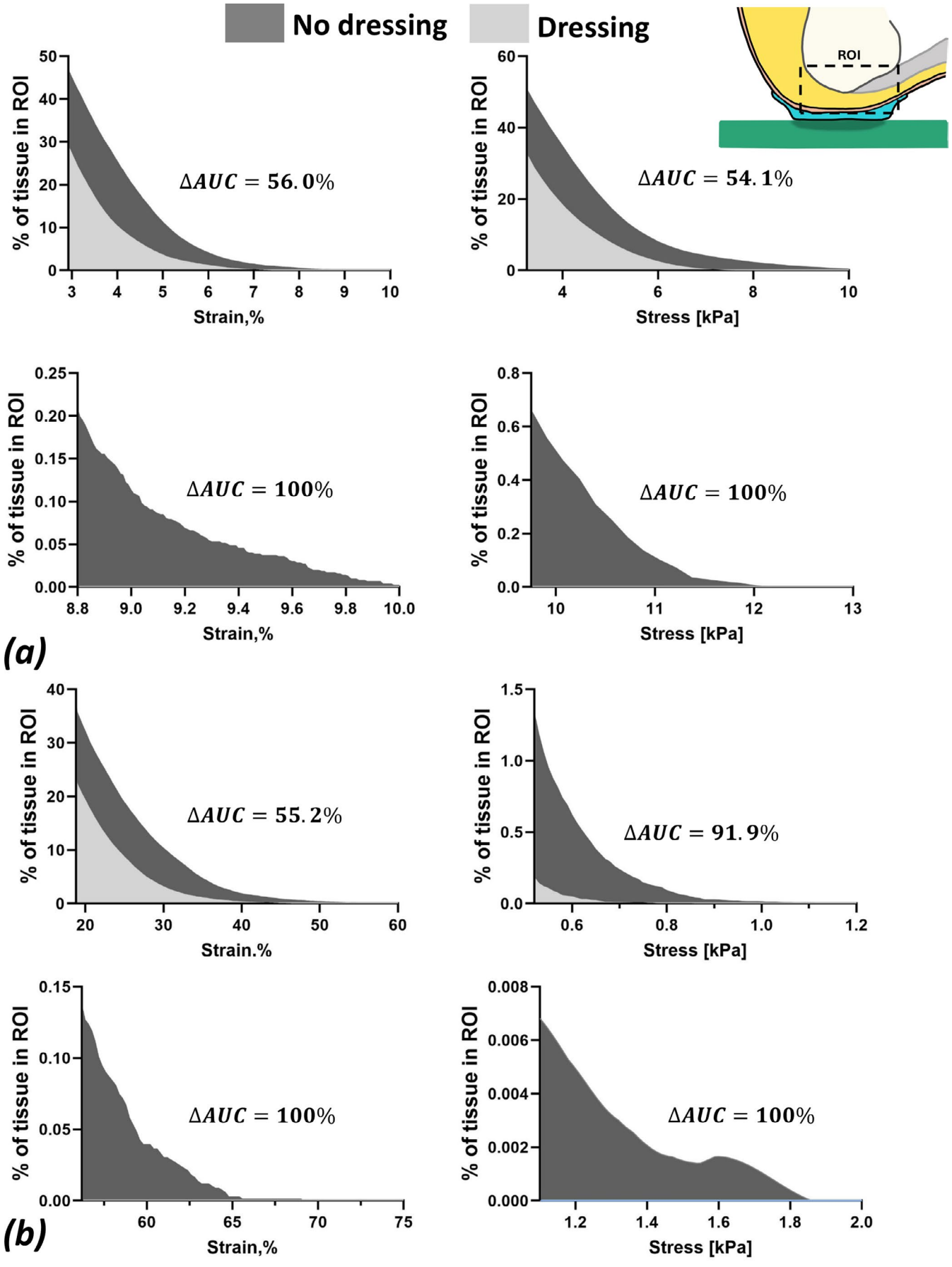

FIGURE 4 | Legend on next page.

FIGURE 4 | Histograms focusing on soft tissue exposure to high strains and stresses, showing (a) skin and (b) adipose tissue exposure to effective strains (left column) and stresses (right column) in the region of interest (ROI). The top row in each panel shows values above the 25th percentile and the bottom row shows values above the 75th percentile. ΔAUC = difference in areas under the curve between the ALLEVYN COMPLETE CARE (Smith & Nephew Limited) dressing and no cases.

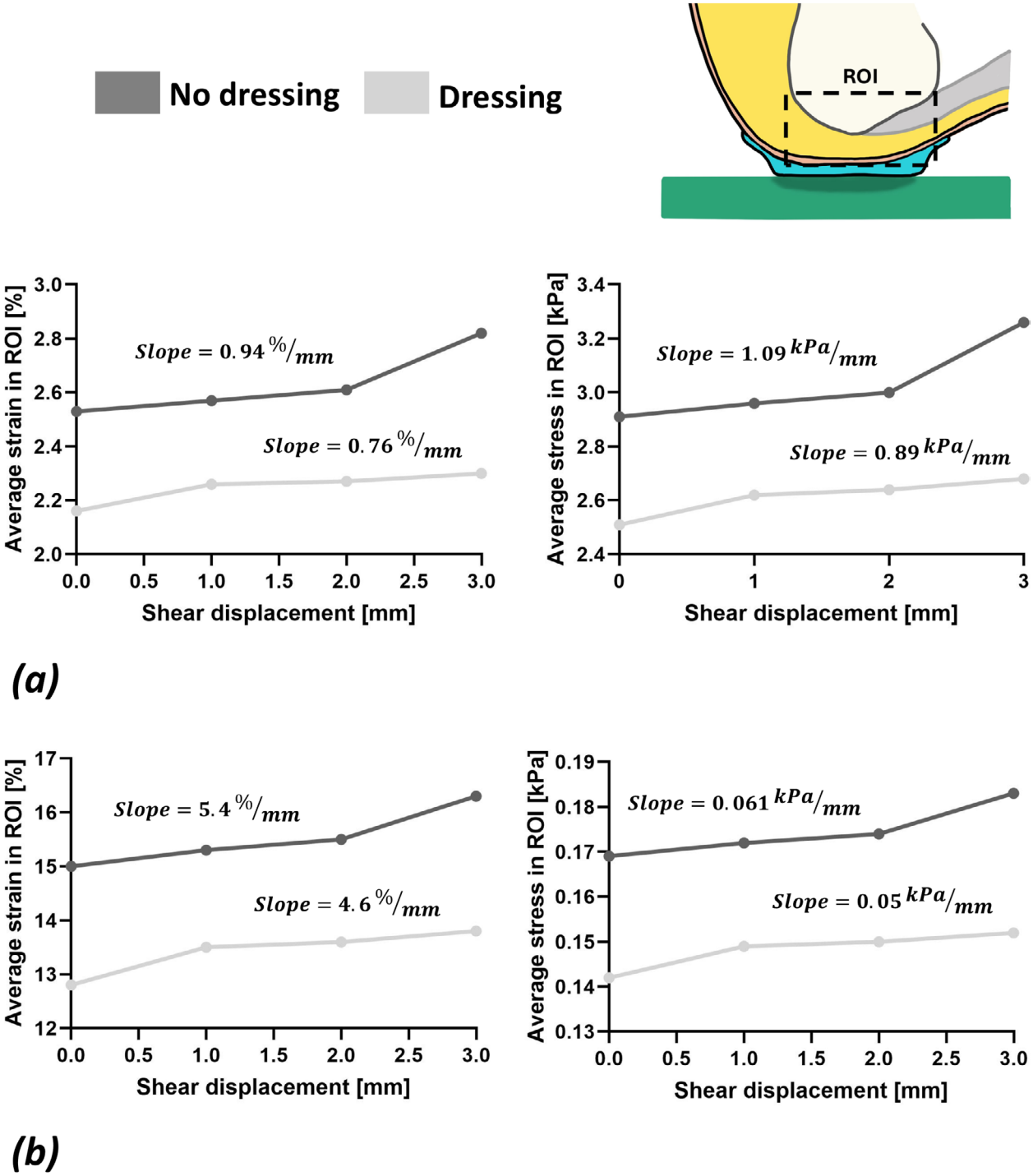

FIGURE 5 | Plots of average maximal principal strain (left column) and stress (right column) values in the soft tissues within the region of interest (ROI), as a function of the extent of shear displacements, comparing the ALLEVYN COMPLETE CARE (Smith & Nephew Limited) dressing to the no-dressing condition, for (a) skin and (b) adipose tissues.

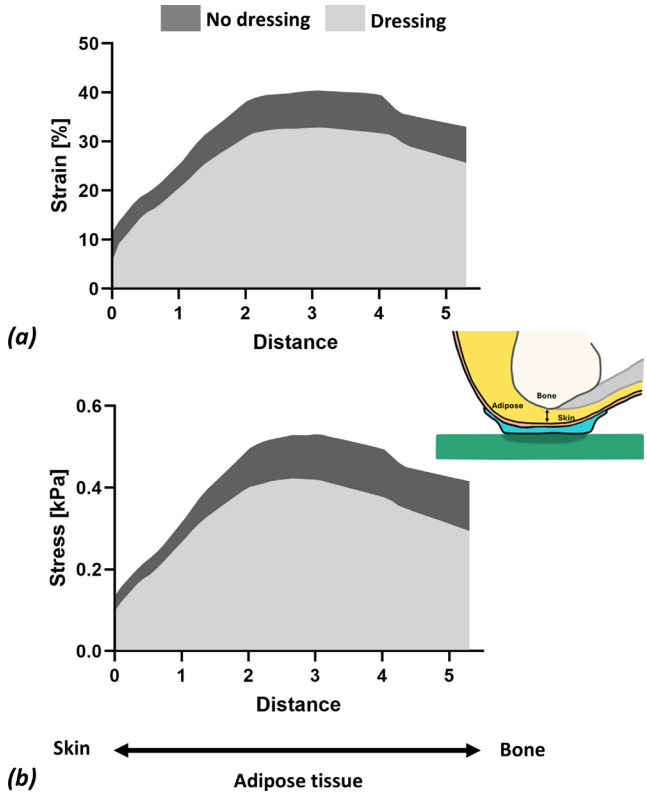

FIGURE 6 | Plots of the effective (a) strain and (b) stress levels along a vertical path crossing the depth of adipose tissue in the posterior heel from the adipose-skin to the adipose-bone interfaces (as marked in the right frame), for the ALLEVYN COMPLETE CARE (Smith & Nephew Limited) dressing versus no cases.

TABLE 4 | The protective efficacy index (PEI) for the tested ALLEVYN COMPLETE CARE dressing.

	PEI (%)	
	Above 25%	**Above 75%**
Strain-based calculation		
Skin	56.0	100
Adipose tissue	55.2	100
Heel soft tissues combined	54.7	100
Stress-based calculation		
Skin	54.1	100
Adipose tissue	91.9	100
Heel soft tissues combined	52.7	100

combination of extremely high FEAE and PEI values, particularly with respect to stress concentrations in the upper quartile, supports the hypothesis that the ACC dressing provides effective biomechanical protection in pressure ulcer prevention.

Notably, the ACC dressing maintained a relatively high COF across its mobile layers, with the mean COFs exceeding 0.6, even under moist conditions (Figure 2a, Table 3). These relatively high layer-on-layer COFs during moist conditions reflect the capacity of this dressing to continue dissipating shear through inter-layer frictional sliding, a critical factor in tissue protection, under potentially moisture-induced softening of the relevant layers. The ACC dressing design hence enables the frictional energy to still be absorbed within the dressing construct whilst it is moist, rather than transferred to the skin, which is important in clinical settings. Additionally, under the induced moisture conditions, the ACC dressing showed increased interlayer displacements, promoting effective shear dissipation during realistic clinical usage durations lasting several days (typically up to 7 days [9]).

One of the standout features of the ACC dressing is its thin and relatively stiff fourth layer, positioned away from the skin, under the masking film (Figure 1b). At only 0.35 mm, this layer is notably thinner than those in comparable dressings, including the previous-generation ALLEVYN LIFE dressing by the same manufacturer. Interestingly, its material possesses stiffness that prevents excessive deformations of the inner dressing layers under mechanical loads, which is consistent with the principle that placing increasingly stiffer layers above a softer, skin-facing layer can help alleviate strain and stress concentrations in the tissues [12]. This contributes to a more uniform distribution of contact forces between the dressing and the support surface and across the inner structure of the dressing, and hence, to minimising focal loads in tissues when these contact forces reach the skin. Additionally, the stiffness of this thin fourth layer enables the dressing to better respond to patient movements involving transfer of shear to the dressing (such as when sliding in bed, repositioning, tossing, spontaneous motions and whilst getting into or out of the bed), as those shear forces cause the stiffer fourth layer to frictionally slide over the underlying third layer whilst maintaining its shape, as opposed to being self-distorted by the external shear. In other words, having a stiffer external layer as in the ACC dressing design promotes and supports the layer-on-layer frictional sliding mechanism for shear dissipation, and ultimately, helps achieve effective PUP.

In many published works, we have demonstrated that the PEI is a powerful metric to quantify the protective performance of dressing types used in PUP, and in various clinical contexts such as intensive care, operating rooms, supine and prone positions, and application to the sacrum, heel, and facial anatomical sites [12, 14–19]. The current PEI data further corroborate the protective advantage offered by the new ACC dressing, quantifying its capacity to alleviate stress and strain concentrations on the skin and subcutaneously (Table 4). In this study, the PEI was calculated separately for stress and for strain, as each of these outcome measures provides complementary biomechanical insights. Specifically, strain describes local tissue deformations directly, whereas stress reflects internal force distributions and is also influenced by the local stiffness of soft tissues and the pressure-related (volumetric) component of loading [22, 28]. Therefore, prophylactic dressing can yield different levels of PEI depending on whether stress or strain is used as the evaluation metric. For example, in adipose tissue above the 25th percentile, the ACC dressing achieved a markedly higher reduction in tissue stress exposure (up to 92%) than in strain exposure (around 55%) (Table 4). This reflects the dressing's capacity to redistribute

internal forces even when the resulting deformations (strains) are less dramatically affected. Reporting both stress- and strain-based PEI values thus provides a more complete characterisation of the protective performance of prophylactic dressings.

The superior FEAE of the ACC dressing (Table 3), which is notably higher than that of ALLEVYN LIFE [9], consistently demonstrates the effectiveness of the ACC dressing in mitigating elevated soft tissue loading exposures. In further direct comparison to ALLEVYN LIFE, the ACC design shows several critical advantages in maintaining biomechanical stability and protective efficacy. The ALLEVYN LIFE dressing, whilst capable of absorbing frictional energy, relies on thicker layers, particularly a 4 mm fourth layer that, whilst offering some protective benefits through cushioning, does not facilitate the extent of layer-on-layer motion that the ACC dressing provides. Already a decade ago, we have demonstrated that cushioning in a single layer is not as effective as the protective interactions that a multi-layer dressing construct of the same total thickness can offer [10]. Although the FEAE measurement method was introduced in our prior work [9], and computational modelling of prophylactic dressings for the heel has been previously performed [10], this study is the first to integrate these two approaches. Specifically, we provide a direct link between empirical FEAE values, measured in a controlled, non-anatomical setup, and the resulting soft tissue load relief observed in an anatomically realistic computational model of the heel. This integration is non-trivial, as it connects device-level mechanical behaviour with its anatomical effects under clinically relevant conditions. Our results demonstrate that a high FEAE value, indicating strong internal shear absorption, correlates with a marked reduction in concentrated soft tissue strains and stresses. Thus, this work contributes novel insight by bridging in vitro frictional energy absorption metrics with in silico anatomical load mitigation, highlighting the translational relevance of FEAE as a predictor of biomechanical efficacy in pressure ulcer/injury prevention.

In the ACC dressing, the contrast stiffness between the thin, stiffer fourth and the more compliant internal layers promotes effective shear dissipation and alleviates focal soft tissue loads through redistribution. This is consistent with our previous findings [10]. Of note, assuming that the dressing is applied to a patient who is already positioned on an adequate support surface providing good immersion and envelopment, the dressing should not protect by a cushioning MOA (as its contribution to pressure redistribution would be minimal to negligible compared to that of the support surface). The primary MOA of a preventative dressing should be in shear mitigation, and, as shown in this work, this is successfully delivered by the ACC dressing.

Importantly, the strain and stress values found in this study, particularly peak principal strains of approximately 20%–30% and von Mises stresses around 10–20 kPa in the heel without protection, are well aligned with previous finite element studies of the posterior heel. For example, Sopher et al. [22] reported strain ranges of 15%–40% in the unprotected heel fat pad, whilst Levy and Gefen [24] demonstrated that application of a multilayer dressing could reduce stress exposure by up to 49%. In our study, the ACC dressing reduced stress exposures above the 25th percentile by up to 92%, effectively eliminating high-stress peaks, highlighting a significant advancement in protective performance.

Although we applied the PEI metric developed by our team, its conceptual basis is closely aligned with recent independent work. Whilst Fougeron and colleagues [20, 21] confirmed the protective benefits of bilayer heel dressings via strain cluster volume analysis, those studies did not assess the effect of inter-layer movements. The present study uniquely contributes to the field by identifying frictional sliding between internal layers as a key mechanism for more effective shear mitigation and stress alleviation in soft tissues protected by the dressing.

The clinical value of this MOA has been evidenced in a recent systematic literature review and meta-analysis of PU incidence amongst at-risk patients, where the previous multi-layer dressing was found to reduce the risk of PUs by 66%, even in the presence of coordinated PUP care bundles [29].

This study contributed to the understanding of MOAs of dressings used for PUP and to the arsenal of contemporary bioengineering laboratory methods capable of quantitatively assessing the prophylactic capacity of dressings in a standardised manner, and yet, several limitations should be acknowledged. Firstly, our in vitro and computational methods, although advanced and robust, may not entirely capture the complex and diverse clinical environments and the individual patient variability, such as differences in anatomy, tissue composition and biomechanical properties across age groups, the body habitus or background medical conditions (such as the impact of degenerative tissue changes, malnourishment or obesity, diabetes, peripheral vascular diseases, etc.). Additionally, both the FEAE and PEI outcomes were assessed under controlled conditions simulating short-term clinical scenarios. These may not fully represent prolonged wear of the dressing, or the impact of non-sweat body fluids such as exposure to urine, faeces or exudate from a nearby wound, or varied atypical patient movement patterns that exist in the real-world settings, which could affect the performance of the studied dressing over extended periods. The nature of the current empirical and computational work imposes certain limitations in terms of generalisability. Specifically, the mechanical energy transfer model used to calculate the FEAE characteristics of the ACC dressing (Appendix A), and the use of a single representative heel anatomy in the in silico simulations (Appendix B), limit direct applicability to patient-specific cases. This is due not only to inter-individual variability in intrinsic factors, such as anatomy, tissue properties, comorbidities, and movement patterns, but also to the large number of potential extrinsic variables in clinical practise. These include differing support surface types, bedframe configurations, head-of-bed elevations, bedsheet materials, and dressing application techniques. Therefore, the reported results should be interpreted as reflecting general trends in the protective performance of the ACC dressing under controlled laboratory and simulated anatomical conditions, rather than quantitative predictions for specific patients or settings.

In conclusion, the ACC dressing exhibited strong protective efficacy through high FEAE and PEI values, demonstrating its potential to reduce the PU risk in relevant clinical settings such as intensive care, surgical, and long-term care facilities. The high FEAE of the ACC dressing, which remains stable under perspiration-induced moisture and repetitive shear exposures, further indicates that this dressing is likely to deliver

a consistent level of protection over the intended multiple-day period of clinical use. Moreover, the in silico PEI studies demonstrated that the ACC dressing design alleviates skin and deep tissue strain/stress concentrations and further eliminates those tissue strain/stress concentrations that are the highest and therefore associated with tissue injury risk. Given these promising laboratory results and the previously reported PUP clinical efficacy of ALLEVYN LIFE dressings [30], it is highly likely that future clinical studies will validate the effectiveness of the second-generation ACC dressing in real-world conditions and for specific at-risk patient groups.

Acknowledgements

Smith & Nephew Limited provided financial funding for this study. Author Amit Gefen is a paid consultant of Smith & Nephew Limited.

Disclosure

The authors declare that they have followed the Wiley best practise guidelines on research integrity and publishing ethics.

Ethics Statement

The authors have nothing to report.

Consent

The authors have nothing to report.

Conflicts of Interest

The authors declare no conflicts of interest other than those stated in the Acknowledgements.

Data Availability Statement

The data that support the findings of this study are available from the corresponding author upon reasonable request.

Endnotes

[1] For a purely elastic material, the stiffness remains constant over time ($E_{ins} = E_{lt}$). A ratio $E_{ins}/E_{lt} > 1$ therefore confirms stress relaxation and the viscoelastic nature of the tested material.

References

1. J. Kottner, J. Cuddigan, K. Carville, et al., "Prevention and Treatment of Pressure Ulcers/Injuries: The Protocol for the Second Update of the International Clinical Practice Guideline 2019," *Journal of Tissue Viability* 28, no. 2 (2019): 51–58, https://doi.org/10.1016/j.jtv.2019.01.001.

2. A. Dube, V. Sidambe, A. Verdon, et al., "Risk Factors Associated With Heel Pressure Ulcer Development in Adult Population: A Systematic Literature Review," *Journal of Tissue Viability* 31, no. 1 (2022): 84–103, https://doi.org/10.1016/j.jtv.2021.10.007.

3. D. Beeckman, A. Fourie, C. Raepsaet, et al., "Silicone Adhesive Multilayer Foam Dressings as Adjuvant Prophylactic Therapy to Prevent Hospital-Acquired Pressure Ulcers: A Pragmatic Noncommercial Multicentre Randomized Open-Label Parallel-Group Medical Device Trial*," *British Journal of Dermatology* 185, no. 1 (2021): 52–61, https://doi.org/10.1111/BJD.19689.

4. E. Hahnel, M. el Genedy, T. Tomova-Simitchieva, et al., "The Effectiveness of Two Silicone Dressings for Sacral and Heel Pressure Ulcer Prevention Compared With no Dressings in High-Risk Intensive Care Unit Patients: A Randomized Controlled Parallel-Group Trial," *British Journal of Dermatology* 183, no. 2 (2020): 256–264, https://doi.org/10.1111/BJD.18621.

5. EPUAP, NPIAP, and PPPIA, *Prevention and Treatment of Pressure Ulcers/Injuries: Clinical Practice Guideline* (EPUAP, NPIAP, PPPIA, 2019).

6. A. Gefen, D. M. Brienza, J. Cuddigan, E. Haesler, and J. Kottner, "Our Contemporary Understanding of the Aetiology of Pressure Ulcers/Pressure Injuries," *International Wound Journal* 19 (2022): 692–704, https://doi.org/10.1111/iwj.13667.

7. C. Greenwood, "Heel Pressure Ulcers: Understanding Why They Develop and How to Prevent Them," *Nursing Standard* 37, no. 2 (2022): 60–66, https://doi.org/10.7748/NS.2021.E11740.

8. K. K. Ceelen, A. Stekelenburg, S. Loerakker, et al., "Compression-Induced Damage and Internal Tissue Strains Are Related," *Journal of Biomechanics* 41, no. 16 (2008): 3399–3404, https://doi.org/10.1016/J.JBIOMECH.2008.09.016.

9. C. Marché, S. Creehan, and A. Gefen, "The Frictional Energy Absorber Effectiveness and Its Impact on the Pressure Ulcer Prevention Performance of Multilayer Dressings," *International Wound Journal* 21, no. 4 (2024): 1–14, https://doi.org/10.1111/iwj.14871.

10. A. Levy, M. B. O. Frank, and A. Gefen, "The Biomechanical Efficacy of Dressings in Preventing Heel Ulcers," *Journal of Tissue Viability* 24, no. 1 (2015): 1–11, https://doi.org/10.1016/j.jtv.2015.01.001.

11. A. Gefen, "Pressure Ulcer Prevention Dressing Design and Biomechanical Efficacy," *Journal of Wound Care* 29, no. Suppl 12 (2020): S6–S15, https://doi.org/10.12968/JOWC.2020.29.SUP12.S6.

12. A. Gefen, "Alternatives and Preferences for Materials in Use for Pressure Ulcer Prevention: An Experiment-Reinforced Literature Review," *International Wound Journal* 19 (2022): 1797–1809, https://doi.org/10.1111/iwj.13784.

13. A. Lustig, P. Alves, E. Call, N. Santamaria, and A. Gefen, "The Sorptivity and Durability of Gelling Fibre Dressings Tested in a Simulated Sacral Pressure Ulcer System," *International Wound Journal* 18, no. 2 (2020): 194–208, https://doi.org/10.1111/iwj.13515.

14. A. Orlov and A. Gefen, "Differences in Prophylactic Performance Across Wound Dressing Types Used to Protect From Device-Related Pressure Ulcers Caused by a Continuous Positive Airway Pressure Mask," *International Wound Journal* 20, no. 4 (2023): 942–960, https://doi.org/10.1111/iwj.13942.

15. M. Lustig and A. Gefen, "The Biomechanical Efficacy of a Dressing With a Soft Cellulose Fluff Core in Protecting Prone Surgical Patients From Chest Injuries on the Operating Table," *International Wound Journal* 19, no. 7 (2022): 1786–1796, https://doi.org/10.1111/IWJ.13783.

16. A. Gefen, M. Krämer, M. Brehm, and S. Burckardt, "The Biomechanical Efficacy of a Dressing With a Soft Cellulose Fluff Core in Prophylactic Use," *International Wound Journal* 17 (2020): 1968–1985, https://doi.org/10.1111/iwj.13489.

17. L. Peko, M. Barakat-Johnson, and A. Gefen, "Protecting Prone Positioned Patients From Facial Pressure Ulcers Using Prophylactic Dressings: A Timely Biomechanical Analysis in the Context of the COVID-19 Pandemic," *International Wound Journal* 17, no. 6 (2020): 1595–1606, https://doi.org/10.1111/IWJ.13435.

18. D. Schwartz and A. Gefen, "The Biomechanical Protective Effects of a Treatment Dressing on the Soft Tissues Surrounding a Non-Offloaded Sacral Pressure Ulcer," *International Wound Journal* 16, no. 3 (2019): 684–695, https://doi.org/10.1111/IWJ.13082.

19. D. Schwartz, A. Levy, and A. Gefen, "A Computer Modeling Study to Assess the Durability of Prophylactic Dressings Subjected to Moisture in Biomechanical Pressure Injury Prevention," *Ostomy/Wound Management* 64 (2018): 18–26, https://doi.org/10.25270/owm.2018.7.1826.

20. N. Fougeron, G. Chagnon, N. Connesson, et al., "Finite Element Tissue Strains Computation to Evaluate the Mechanical Protection Provided by a New Bilayer Dressing for Heel Pressure Injuries," *Advances in Skin & Wound Care* 36, no. 10 (2023): 549–556, https://doi.org/10.1097/ASW.0000000000000042.

21. N. Fougeron, N. Connesson, G. Chagnon, et al., "New Pressure Ulcers Dressings to Alleviate Human Soft Tissues: A Finite Element Study," *Journal of Tissue Viability* 31, no. 3 (2022): 506–513, https://doi.org/10.1016/j.jtv.2022.05.007.

22. R. Sopher, J. Nixon, E. McGinnis, and A. Gefen, "The Influence of Foot Posture, Support Stiffness, Heel Pad Loading and Tissue Mechanical Properties on Biomechanical Factors Associated With a Risk of Heel Ulceration," *Journal of the Mechanical Behavior of Biomedical Materials* 4 (2011): 572–582, https://doi.org/10.1016/j.jmbbm.2011.01.004.

23. A. Levy, K. Kopplin, and A. Gefen, "Simulations of Skin and Subcutaneous Tissue Loading in the Buttocks While Regaining Weight-Bearing After a Push-Up in Wheelchair Users," *Journal of the Mechanical Behavior of Biomedical Materials* 28 (2013): 436–447, https://doi.org/10.1016/j.jmbbm.2013.04.015.

24. A. Levy and A. Gefen, "Computer Modeling Studies to Assess Whether a Prophylactic Dressing Reduces the Risk for Deep Tissue Injury in the Heels of Supine Patients With Diabetes," *Ostomy/Wound Management* 62 (2016): 42–52.

25. B. E. Keenan, S. L. Evans, and C. W. J. Oomens, "A Review of Foot Finite Element Modelling for Pressure Ulcer Prevention in Bedrest: Current Perspectives and Future Recommendations," *Journal of Tissue Viability* 31, no. 1 (2022): 73–83, https://doi.org/10.1016/j.jtv.2021.06.004.

26. S. S. Loerakker, S. Loerakker, A. Stekelenburg, et al., "Temporal Effects of Mechanical Loading on Deformation-Induced Damage in Skeletal Muscle Tissue," *Annals of Biomedical Engineering* 38, no. 8 (2010): 2577–2587, https://doi.org/10.1007/S10439-010-0002-X.

27. A. Orlov, A. Lustig, A. Grigatt, and A. Gefen, "Fluid Handling Dynamics and Durability of Silver-Containing Gelling Fiber Dressings Tested in a Robotic Wound System," *Advances in Skin & Wound Care* 35, no. 6 (2022): 326–334, https://doi.org/10.1097/01.ASW.0000823972.16446.ff.

28. G. Holzapfel, *Nonlinear Solid Mechanics. A Continuum Approach for Engineering* (John Wiley & Sons, 2000).

29. L. Atkinson and B. Costa, *Pressure Injury Prevention With a Unique Multi-Layer Foam Dressing: A Systematic Review and Meta-Analysis of Randomized Controlled Trials* (EPUAP, 2024).

30. C. Forni, F. D'Alessandro, P. Gallerani, et al., "Effectiveness of Using a New Polyurethane Foam Multi-Layer Dressing in the Sacral Area to Prevent the Onset of Pressure Ulcer in the Elderly With Hip Fractures: A Pragmatic Randomised Controlled Trial," *International Wound Journal* 15, no. 3 (2018): 383–390, https://doi.org/10.1111/IWJ.12875.

Appendix A

Frictional Energy Absorber Effectiveness (FEAE) Calculations

The FEAE testing method quantifies how effectively a multilayer dressing can dissipate mechanical energy by inter-layer frictional sliding relative to the compressive work done on the same dressing.

$$FEAE = \frac{W_{\text{friction}}}{W_{\text{compression}}} \tag{A1}$$

In energy terms, for a dressing with internal interfaces $i, i+1$ (in the current work: interfaces 2,3 and 3,4), the frictional sliding work is approximated as:

$$W_{\text{friction}} = \sum_i \mu_{i,i+1} N \left| d_{i,i+1} \right| \tag{A2}$$

where $\mu_{i,i+1}$ is the coefficient of friction between the two layers, $d_{i,i+1}$ is their relative sliding displacement (along with the shear direction), and N is the normal force transmitted through the dressing during the test.

The compressive work on the dressing is:

$$W_{\text{compression}} = N\Delta h = N\varepsilon h \tag{A3}$$

with h being the undeformed dressing thickness and ε is the engineering compressive strain. Dividing the two eliminates the dependence on N, giving a practical calculation:

$$FEAE = \frac{\sum_i \mu_{i,i+1} \left| d_{i,i+1} \right|}{\varepsilon h} \tag{A4}$$

The FEAE is computed per unit area, so it does not depend on the contact area of the dressing with skin or with the support surface, and furthermore, does not require considering a full three-dimensional (3D) stress field. Accordingly, the inputs are obtained from two-dimensional (2D) measurements, namely, (i) the in-plane interlayer sliding, which is measured per internal interface in a central, longitudinal cross-section through the dressing along the shear direction, and (ii) the compressive strain which is the thickness reduction of the dressing in the same cross-sectional plane. Given that the contribution of the area parameter is cancelled through the formulation and the inputs are all in-plane, the FEAE calculation does not require 3D analyses.

The inputs and experimental workflow to obtained the FEAE are as follows:

1. Coefficients of friction $\mu_{i,i+1}$ are measured by means of an electronically controlled tilting-table tribometer, under a representative pressure of 30 mmHg. The onset angle of sliding yields the μ for each interface (here: 2,3, 3,4), per each test condition (e.g., dry specimen simulating out-of-package versus moist specimen simulating a used dressing).
2. Inter-layer sliding $d_{i,i+1}$ and compressive strain ε are measured in a combined compression-shear apparatus: the dressing is compressed (by a 1.1 kgf) and sheared up to the pre-sliding force. Digital image correlation (DIC) tracks markers in each layer to obtain the $d_{i,i+1}$ at the target shear force, and the thickness change Δh yields $\varepsilon = {}^{\Delta h}/_{h}$. The relative layer displacements were recorded at the maximum shear force before sliding (which was approximately 6 N). These displacements were measured optically using a high-resolution DSLR camera, with fiducial markers sprayed on the layer cross-section and tracked using a DIC algorithm implemented in a custom MATLAB programme. This method captures the relative sliding of one layer versus the adjacent ones, independent of the overall specimen movement. Accordingly, the experimental measurements were referenced to the shear force at slip onset under a controlled compressive load, whereas the finite element simulations used displacement-controlled boundary conditions. This difference was intentional: In the test rig, shear forces were measured directly whereas in the computational model, displacements were prescribed to reproduce the equivalent kinematic state (i.e., heel compression and shear just before slip). What is compared between the two is not the absolute force or displacement, but the relative sliding between layers under clinically relevant loads, which is largely independent of the loading path once the pre-slip state is reached. Although force- and displacement-control can produce different reaction forces if the boundary stiffness changes, the local kinematics of inter-layer motion and the mechanical energy-dissipating behaviour of the dressing remain robust.
3. The quantities $\mu_{2,3}, \mu_{3,4}, d_{2,3}, d_{3,4}, h, \varepsilon$ were substituted into Equation (A4) to compute the FEAE. The results may also be expressed as a percentage (×100).

The values of the COF $\mu_{i,i+1}$ measured for each of the 6 samples per interface and condition combinations are reported in Table A1. The vertical compression y and the displacements $d_{i,i+1}$ used to calculate the FEAE according to Equation (A4) are specified in Table A2.

To ensure the validity of group comparisons for the interlayer coefficient of friction $\mu_{i,i+1}$ and displacement $d_{i,i+1}$ data, we tested the residuals from each group for normality using the Shapiro–Wilk test. As shown in Table A3, no significant departures from normality were detected (all $p > 0.05$). The sample groups were balanced ($n = 6$ per condition) and independent, supporting the use of one-way ANOVA and Tukey–Kramer post hoc comparisons for statistical analysis.

TABLE A1 | Means and standard deviations of the coefficient of friction for dry and moist dressing specimens.

Condition		Interface 2,3		Interface 3,4	
		Average	SD	Average	SD
New	Dry	0.79	0.03	0.98	0.02
Used	Moist	0.72	0.06	0.61	0.05

TABLE A2 | Compression, displacement and resulting FEAE values for all the dry and moist dressing specimens. Mean values are provided in bold font.

Specimen	Conditioning		Compression (mm)	Interface 2,3 (mm)	Interface 3,4 (mm)	FEAE (%)
1	New	Dry	1.31	0.51	1.01	106
2			1.35	0.50	0.85	91
3			1.21	0.53	0.67	88
4			1.22	0.56	0.75	96
5			1.21	0.41	0.88	97
6			1.10	0.42	1.07	125
Mean			**1.23**	**0.49**	**0.87**	**100**
Standard deviation			0.09	0.06	0.15	13
1	Used	Moist	0.98	0.58	0.82	94
2			1.32	0.81	1.23	100
3			1.42	0.71	1.23	89
4			1.25	0.66	1.03	88
5			1.28	0.66	1.13	91
6			1.28	0.62	1.30	97
Mean			**1.26**	**0.67**	**1.12**	**93**
Standard deviation			1.15	0.08	0.18	5

TABLE A3 | The Shapiro–Wilk test results for displacement and coefficient of friction (COF) measurements at interfaces 2–3 and 3–4 under new and used dressing conditions.

Main variable	Dressing condition	$W_{2,3}$	$W_{3,4}$	$p_{2,3}$	$p_{3,4}$	Normality assumption met
Displacement	New	0.89	0.97	0.37	0.89	Yes
	Used	0.94	0.90	0.65	0.39	Yes
Coefficient of friction	New	0.81	0.85	0.10	0.16	Yes
	Used	0.89	0.94	0.31	0.68	Yes

Appendix B

Protective Efficacy Index Calculations

We calculated two exposure metrics per condition, namely, the maximal principal strain (%) and the von Mises stress (kPa). For each such metric we generated an elementwise distribution over the ROI volume and computed the area under the curve (AUC) of the obtained distribution. We further analysed the AUC data after applying two threshold levels. Specifically, '≥ 25%' means that we only included elements in the ROI for which the strain/stress value was at least 25% of the maximum respective strain/stress value obtained for that specific simulation case. These analyses were termed 'moderate-to-high' strain/stress exposures. Similarly, we applied a higher threshold, '≥ 75%' which indicates that we only included elements for which the strain/stress value was at least 75% of the maximum ('high' strain/stress exposures). The PEI quantifies the alleviation in the tissue strain/stress exposure induced by the dressing relative to the no-dressing condition:

$$\mathrm{PEI}\,(\%) = 100 \times \frac{\mathrm{AUC_{ND}} - \mathrm{AUC_{ACC}}}{\mathrm{AUC_{ND}}} \tag{B1}$$

The PEI is computed separately for each tissue type (i.e., skin and adipose tissues), as well as for skin and adipose tissues considered together (i.e., the entire ROI). The strain-based calculations are repeated for stress to obtain both strain-based and stress-based PEI measures at the three AUC ranges (the full strain/stress range: zero to 100%, the data subset ≥ 25%, and the data subset ≥ 75%). The PEI values were derived directly from the AUC data reported in Table B1 by means of Equation (B1).

TABLE B1 | Area under the curve (AUC) data for the ALLEVYN COMPLETE CARE (ACC) dressing.

	No dressing	ACC
Strain-based calculation		
Full strain range (0%–100%)		
Skin	292.4	232.6
Adipose tissue	1665.0	1391.0
Heel soft tissues combined	958.5	798.7
Strain data subset ≥ 25%		
Skin	68.0	29.9
Adipose tissue	305.7	136.9
Heel soft tissues combined	150.1	68.0
Strain data subset ≥ 75%		
Skin	0.1	0
Adipose tissue	0.4	0
Heel soft tissues combined	0.2	0
Stress-based calculation		
Full stress range (0%–100%)		
Skin	339.0	270.7
Adipose tissue	18.7	15.4
Heel soft tissues combined	183.6	146.0
Stress data subset ≥ 25%		
Skin	82.5	37.9
Adipose tissue	0.1	0.01
Heel soft tissues combined	46.5	21.9
Stress data subset ≥ 75%		
Skin	0.5	0
Adipose tissue	0	0
Heel soft tissues combined	0.4	0

Appendix C

Deformation of the Support Surface

To assess whether the support surface deformed appreciably under the simulated heel loading, we examined the displacement field of the support surface using focused contour plots and line profiles. As the simulation was performed using displacement-controlled boundary conditions, most of the imposed 4 mm vertical displacement was absorbed by the dressing and heel soft tissues. Accordingly, only a small fraction of the loading was transmitted to the support surface.

The vertical displacement (U_2) and contact pressure maps of the support surface under the posterior heel are shown in Figure C1. These results demonstrate that the support surface experienced a localised vertical compression of approximately 0.35–0.4 mm beneath the centre of the heel footprint, which corresponds to ~4% deformation of the 10 mm-thick support layer. Displacements rapidly decayed outside this central contact zone.

Although no direct measurements of support compression were made during the FEAE experiments, visual inspection showed minimal settlement during testing. This is consistent with the simulation findings and supports the mechanical plausibility of the boundary condition assumptions used in the model.

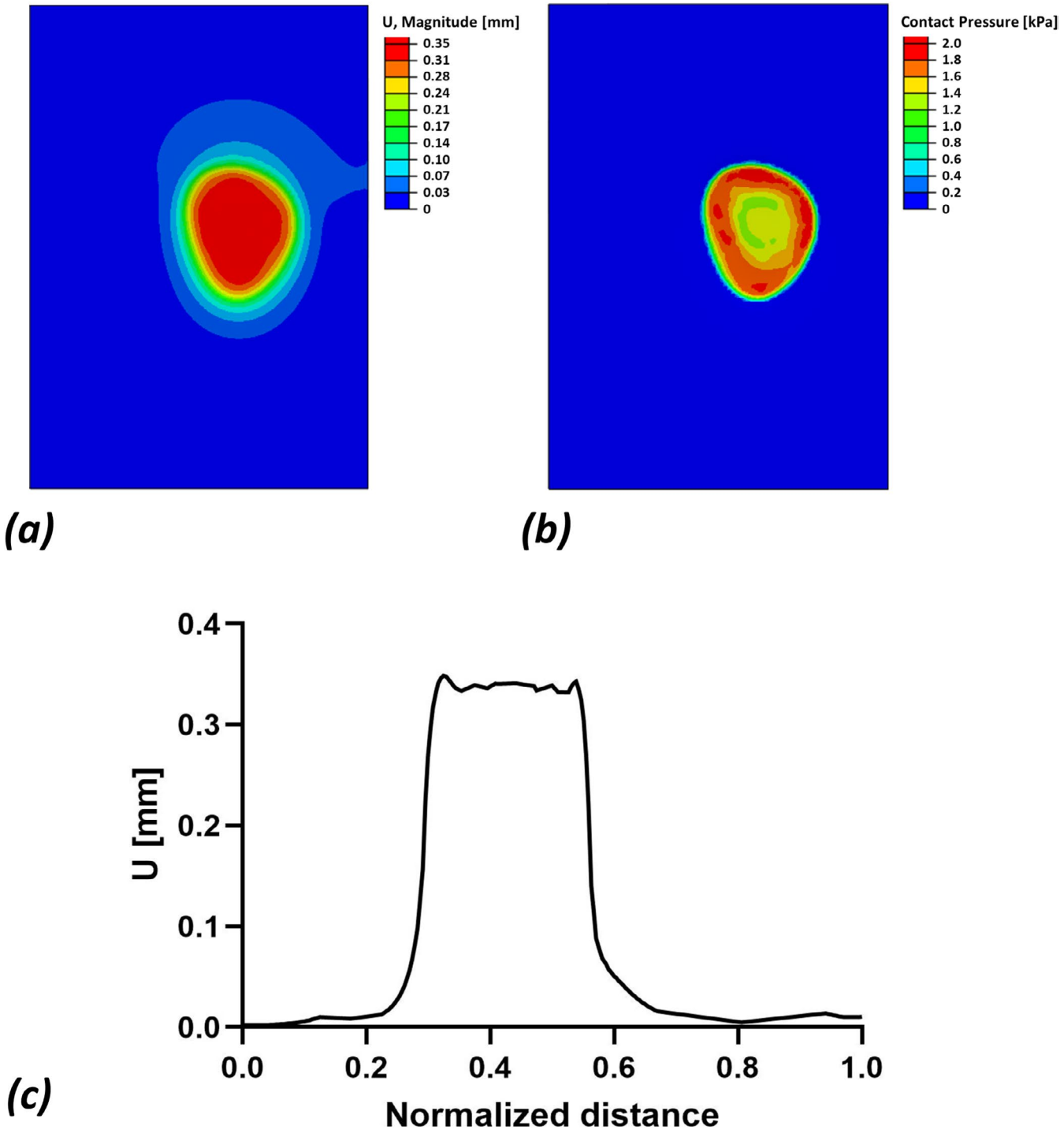

FIGURE C1 | Finite element simulations of the loading state of the support surface beneath the heel: (a) Distribution of the displacements ('U') in mm; (b) Contact pressures on the support surface under the heel, showing the localised footprint of the posterior heel whilst resting on the support surface; (c) Profile of the displacements of the support surface along a centreline across the aforementioned footprint, with the horizontal axis showing normalised distance (0–1) along the path. The maximum surface deformation is approximately 4% (surface displacement of ~0.35 mm from an undeformed 10 mm thickness). The displacement of the surface is shown to decay rapidly outside the heel-support surface contact region.

Appendix D

Slope Analysis of Strain and Stress Trends Under the Shear Displacement Range

To assess how tissue loading evolves under increasing shear, we computed the linear slope of the average maximal principal strain and von Mises stress in the ROI over the 0–3 mm displacement range (Figure D1). This analysis was performed separately for each tissue type (skin, adipose) and for each condition (no dressing versus the applied ACC dressing), using least-squares linear regression. The computed slopes, along with their SE and 95% CIs, are provided in Table D1. Results showed that: (i) In skin, both strain and stress slopes under the ACC dressing were close to zero (95% CI includes zero), indicating flat or near-flat trends. (ii) In adipose tissue, strain increased more rapidly in the 'no dressing' condition compared to the ACC condition, whilst stress slopes remained small in both conditions.

To evaluate whether the slope differences between conditions were statistically significant, we used extra-sum-of-squares *F*-tests (ANCOVA). Although the ACC dressing consistently yielded lower slope point estimates across all the comparisons that were made, none of the differences reached statistical significance (all $p > 0.05$), likely due to the limited displacement range and small effect sizes. These results quantitatively support the interpretation that the ACC dressing slows the rate of strain and stress accumulation during shear displacements, consistent with its frictional energy-absorbing mechanism.

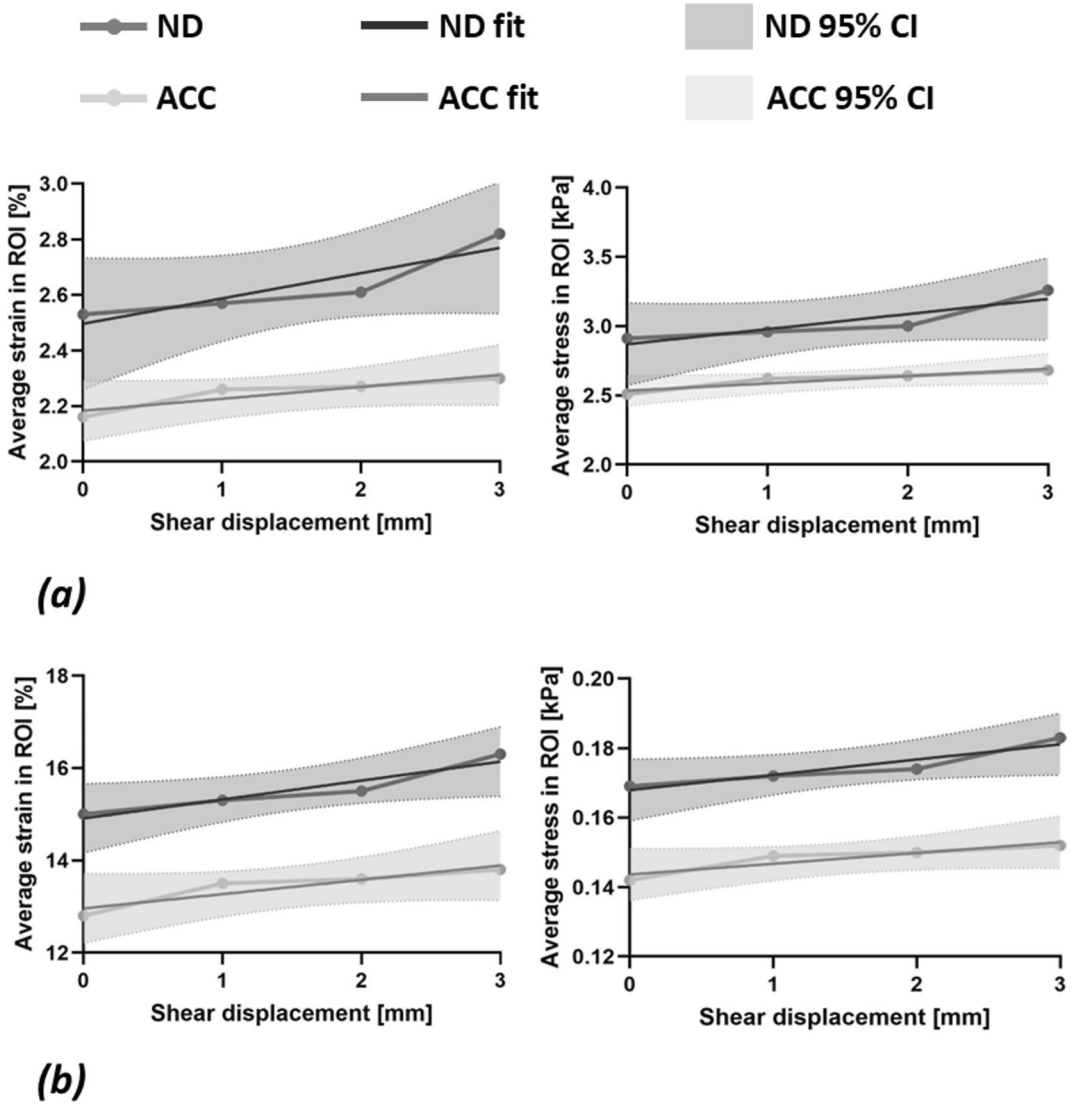

FIGURE D1 | Tissue strain and stress responses in the ROI to an incrementally increasing shear displacement with the ALLEVYN COMPLETE CARE (ACC) dressing and with no dressing (ND), for (a) skin and (b) adipose tissue. Points represent the mean values, solid lines are linear fits and shaded bands are the 95% confidence intervals of the mean fit (dark = ND, light = ACC).

TABLE D1 | Slopes of the linear regression lines for tissue strain and stress responses to a shear displacement (see Figure D1 for additional information).

Tissue type	Measure	Condition	Slope	SE	95% CI
Skin	Strain	ND	0.09	0.03	−0.04 to 0.22
		ACC	0.04	0.01	−0.015 to 0.10
	Stress	ND	0.11	0.04	−0.05 to 0.27
		ACC	0.05	0.01	−0.005 to 0.11
Adipose	Strain	ND	0.41	0.09	0.0087 to 0.81
		ACC	0.31	0.09	−0.091 to 0.71
	Stress	ND	0.004	0.001	−0.0003 to 0.009
		ACC	0.003	0.001	−0.0009 to 0.007

Note: The slopes of the linear regression lines are provided per tissue type and condition.
Abbreviations: ACC, studied dressing; ND, no dressing.